

FAST DIGITAL FEEDBACK SYSTEM FOR ENERGY AND BEAM POSITION STABILIZATION*

R. Dickson, V. A. Lebedev[#], Jefferson Lab, Newport News, VA

Abstract

A digital fast feedback system for beam energy and position stabilization at the target of the CEBAF accelerator is capable of suppressing beam motion in the frequency band from 0 to 80 Hz and also performs narrow band suppression at the first twelve power line harmonics. The system utilizes two VME computers and runs at a 2.4 kHz sampling rate. The numerical algorithm is based on a recursive digital filter with an additional feedforward loop for suppression of high power line harmonics. The system suppresses beam motion by a factor greater than ten, thus achieving the stabilization of relative beam energy fluctuations to better than 10^{-5} and stabilization of beam position on the target to better than 20 μm .

1. INTRODUCTION

Study of the beam motion at different locations in the CEBAF accelerator [1] has shown that the beam has excursions in energy and in both transverse planes. The amplitude of the motion is roughly the same along the machine and is about $(0.5 - 2) \cdot 10^{-4}$ for relative energy change and 0.2 - 0.5 mm for transverse beam motion. The motion spectral density can be separated into two main regions: the low frequency region (0 - 80 Hz), and the high frequency region (below 1 kHz) where the beam motion mainly occurs at power line harmonics. The first three power line harmonics make the main contribution to beam motion at short time intervals, ≤ 1 min, while the contribution from harmonics higher than 12 can be neglected. The sources of the perturbation are scattered along the entire machine and it is almost impossible to correct them locally for each of 320 superconducting cavities and 1800 magnets.

While such beam motion does not cause a problem for beam transport, many experiments require better accuracy for beam energy and position stabilization on the target. A digital beam based feedback system has been chosen as the best candidate to resolve the problem. Such a system has significantly better flexibility than an analog system, and did not require significant changes in hardware.

2. CHOICE OF THE SYSTEM

Achieving the best possible beam stabilization in the framework of existing hardware was the main requirement

*Work was supported by U.S. D.O.E. contract #DE-AC05-84ER40150.

[#] Email: lebedev@jlab.org

we set for the system. SEE beam position monitors (BPM) [2] were already installed for the beam lines of two experimental halls which required beam stabilization. The BPM resolution is about 20 μm per single measurement for beam current more than 10 μA and grows approximately inversely proportionally to the current below 10 μA . Maximum sampling rate determined by the BPM hardware is about 3 kHz. As can be seen below, that implies that the resolution of BPM measurements is a significant factor in determining the beam stabilization.

2.1. Beam Line Optics

The layout of the accelerator is shown in Figure 1. The beam starts in the injector. After acceleration to a required pass number, a fraction of the beam (or the whole beam) can be split by RF separator and sent to one of three experimental halls. Normally the beam is simultaneously delivered to all three experimental halls.

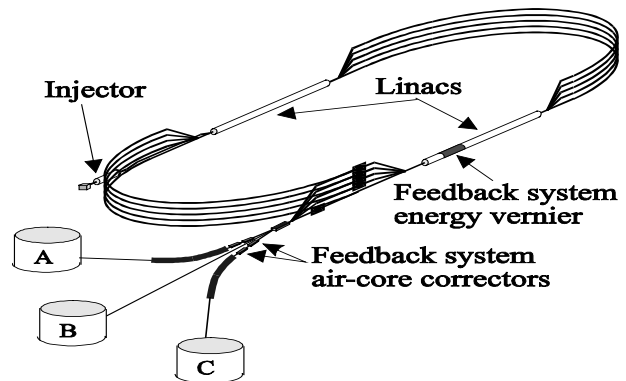


Figure 1: Layout of CEBAF recirculator.

Fast feedback systems are installed in the lines leading to Halls A and C. Each system consists of actuators (energy corrector, two horizontal and two vertical correctors) and a set of responders (BPMs) installed down-stream of the actuators. Taking into account that both halls have common energy regulation, only one of them can be used for energy stabilization. Each beam line has a string of dipoles bending the beam horizontally by 37.5 deg with achromatic optics. The bending creates the dispersion, which allows us to perform the energy stabilization. The beam position change at the responders can be expressed through optical functions of the transfer line and values of actuators,

$$\mathbf{x} = \mathbf{A}\mathbf{c} \quad (1)$$

Here \mathbf{x} is the vector of BPM measurements $\mathbf{x}^T = (x_1, \dots, x_N)$, and \mathbf{c} is the vector of corrections $\mathbf{c}^T = (c_1, \dots, c_M)$. To get a single solution for vector \mathbf{c} , the number of responders

should be more than or equal to the number of actuators, $N \geq M$. Below we will consider a system with four transverse correctors, c_1, c_2, c_3, c_4 and, if the energy correction is on, the energy corrector c_5 . To compute values of actuators which will minimize the beam displacement the SVD (single value decomposition) algorithm [3] is used, so that

$$\mathbf{c} = \mathbf{B}\mathbf{x} \quad , \quad (2)$$

$$\mathbf{B} = (\mathbf{A}^T \mathbf{A})^{-1} \mathbf{A}^T \quad . \quad (3)$$

To achieve maximum resolution the optics of the beam lines was altered. First, the focusing inside arcs was changed to attain maximum dispersion, which is compatible with achromatic transport. Second, the beta-functions through the arcs were adjusted to obtain optimum phase advances in between correctors and active BPMs. To maximize the sampling frequency only five BPM positions (three horizontal and two vertical) are usually used. In this case the optimum betatron phase advance is $\pi(n + 1/2)$ for each pair of correctors and each pair of BPMs. The horizontal beta-function for the third horizontal BPM, which sits at the top of the dispersion function, was reduced to achieve better energy resolution. It yields a momentum resolution of $6.6 \cdot 10^{-6}$ for 20 μm BPM resolution. The use of all BPMs of the arc (six horizontal and six vertical) improves the system resolution by only about 10%. That justifies the reduced set of BPMs.

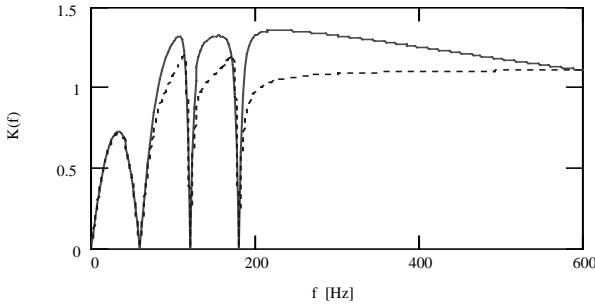


Figure 2: Dependence of the transfer function on frequency; the sampling frequency is 2.4 kHz, the low pass filter bandwidth is 1.5 kHz, $k_0=0.07$, $|k_1|=0.05$, $|k_2|=0.01$, $|k_3|=0.01$, $\arg(k_1)=0$, $\arg(k_2)=0.5$, $\arg(k_3)=0.5$; dashed line - the uncorrected transfer function, solid line - the transfer function corrected for low pass filter bandwidth.

2.2. Digital Filter

Noise in measurements causes the system to excite undesirable beam motion. For a generic single channel feedback system the noise drives the beam motion equal to

$$\overline{x_{output}^2} = \frac{x_{meas}^2}{\pi f_s} \int_0^{\pi f_s} |\mathbf{K}(\omega) - 1|^2 d\omega \quad , \quad (4)$$

where f_s is the sampling frequency, $\overline{x_{meas}^2}$ is the single measurement accuracy, and $\mathbf{K}(\omega)$ is the transfer function

for a harmonic signal, $\mathbf{K}(\omega) = x_{output \omega} / x_{input \omega}$.

The condition of the system stability also imposes a limitation for $\mathbf{K}(\omega)$,

$$\frac{1}{\pi f_s} \int_0^{\pi f_s} \text{Re}(\mathbf{K}(\omega)) d\omega = 1 \quad . \quad (5)$$

This implies that if at some frequency the system strongly suppresses the input signal, $|\mathbf{K}(\omega)| \ll 1$, it should amplify the signal at a different frequency, $|\mathbf{K}(\omega)| > 1$. Thus to achieve optimum system performance, one needs to suppress the beam motion only in frequency ranges where the motion spectral density is significant.

The choice of digital filter parameters has been determined by necessity to suppress the beam motion at low frequency and the first three power line harmonics,

$$\begin{aligned} \mathbf{K}(\omega) &= \frac{e^{i\omega T} - 1}{e^{i\omega T} - (1 - k_0)} \\ &= \prod_{n=1}^3 \frac{e^{i\omega T} - e^{in\omega_1 T}}{e^{i\omega T} - (1 - k_n) e^{in\omega_1 T}} \frac{e^{i\omega T} - e^{-in\omega_1 T}}{e^{i\omega T} - (1 - k_n^*) e^{-in\omega_1 T}} \quad , \quad (6) \\ &\equiv \frac{e^{i\omega T} - \sum_{k=0}^6 a_k e^{-ik\omega T}}{e^{i\omega T} - \sum_{k=0}^6 (a_k + b_k) e^{-ik\omega T}} \end{aligned}$$

where $*$ denotes complex conjugation, $\omega_1 = 2\pi \cdot 60$ Hz, k_0 and $|k_n|$ are the system gains at zero and first three power line harmonics, $\arg(k_n)$ are the gain angles and coefficients a_n and b_n are determined by expanding the numerator and denominator of the first part of the equation into a series. An example of $\mathbf{K}(\omega)$ is shown in Figure 2. A numerical algorithm realizing the transfer function of Eq. (6) can be written in the following form

$$\mathbf{c}_{k+1} = \sum_{n=0}^6 (a_n \mathbf{c}_{k-n} + b_n \mathbf{y}_{k-n}) \quad , \quad (7)$$

where \mathbf{c}_k is the vector of corrections at step k ,

$$\mathbf{y}_k = \mathbf{B}\mathbf{x}_k \quad (8)$$

is the state vector at step k , and \mathbf{x}_k is the vector of measurements at step k .

3. SYSTEM IMPLEMENTATION AND EXPERIMENTAL RESULTS

The system layout is shown in Figure 3. To maximize speed, all digital hardware is concentrated in one VME crate. The system utilizes two CPUs. The first CPU runs the feedback system algorithm and the second provides system control and interface with operators using EPICS software [4]. ADC data acquisition is triggered by the timing module, which sets a series of pulses for multiplexing BPM electrodes. The measurement results are stored in ADC memory and are read after measurement

completion. The timing module is driven by the frequency multiplier, which is phase locked to the power line and creates a series of pulses at a desired power line harmonic. Normally the 40th harmonic (2.4 kHz) is used.

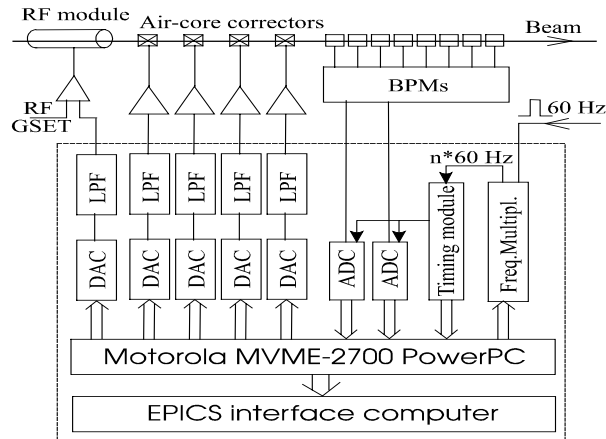


Figure 3: Feedback system schematic

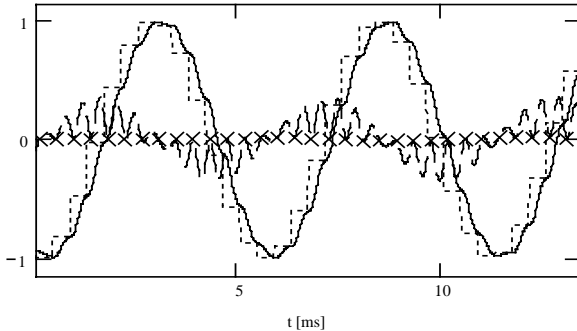


Figure 4: Time domain signals to suppress 180 Hz harmonic perturbation; dotted line - DAC voltage, solid line - post filter correcting signal, dashed line - residual beam motion increased by three times; crosses show beam positions at data acquisition time. The system parameters are similar to Figure 2.

Different halls use different types of BPMs. Hall A uses BPMs with data acquisition time of $2.7 \mu\text{s}$ per electrode. To reduce measurement noise every electrode is read eight times. That yields a total data acquisition time of about $90 \mu\text{s}$. To accelerate data transfer into the computer memory, Direct Memory Access (DMA) is used. This allows reading of data from one ADC in about $70 \mu\text{s}$. The CPU starts calculations of beam positions measured by the first ADC while DMA supplies measurement results of the second ADC. Hall C has BPMs with 16 times longer integration time. This yields a total data acquisition time of about $200 \mu\text{s}$, and only one reading of each electrode is used. That reduces data flux and allows one to avoid DMA transfer.

After data acquisition is performed, the system computes the required corrections and writes new corrector values into the DACs. Analog low pass filters are used to smooth DAC voltage. Reducing the filter cutoff frequency allows one to get a better approximation of a sinusoid, but is limited by system instability. Usually a bandwidth of

1.5 kHz is used. Figure 2 demonstrates the effect of filter bandwidth on the transfer function. It is important to note that although for the first three power line harmonics the system perfectly conceals the beam motion at the time when data acquisition is performed, it fails to conceal it in between data acquisitions. This is because the sinusoid is approximated by DAC voltage with finite accuracy. Figure 4 demonstrates this for 180 Hz beam motion. As one can see, the suppression factor is only about ten.

To improve the suppression of beam motion for the first three power line harmonics and suppress higher harmonics, a feedforward system was built on the top of the feedback system. To implement it the DACs are run at a frequency three times higher than the data acquisition from the BPMs. DAC corrections are summed from the feedback system predictions and data coming from a circular feedforward array. The length of the feedforward array is set such that after one power line period, the feedforward array is completely traversed. To match DAC and ADC frequencies, every feedback system prediction is propagated for three consecutive DAC corrections. Computation of the feedforward array data is performed by a UNIX process which reads time domain data from the correctors and BPMs, computes amplitudes and phases of power line harmonics present in the beam motion, and then calculates time domain signals for the feedforward array. The amplitudes and phases of power line harmonics are relatively stable, and therefore good suppression for the first twelve power line harmonics is achieved with comparatively modest sampling frequency. Figure 5 demonstrates the beam motion spectrum with the system on.

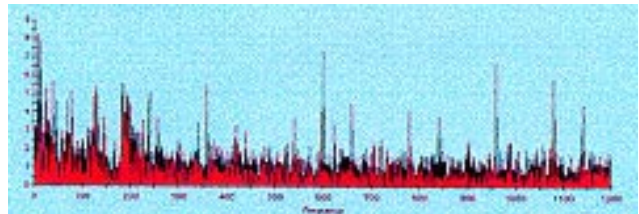


Figure 5: Spectrum of the beam motion with fast feedback system on in frequency range of $0 - 1.2 \text{ kHz}$. If the system is off, the amplitude of the first power line harmonic is about 30 times the vertical scale.

Authors are grateful to A. Hutton for his continuous support of this work. We also would like to thank J. Bisognano, L. Harwood, and M. Tiefenback for useful discussion.

4. REFERENCES

- [1] D. Douglas, *et al.*, CEBAF-PR-89-008; *Proc. of the 1989 Particle Accelerator Conference*, pp. 557-559 (1989).
- [2] T. Powers, *Proc. of the 1998 Beam Inst. Workshop*, pp. 256-265.
- [3] W. Press, B. Flannery, *et al*, *Numerical Recipes in C*, Cambridge University Press, 1988.
- [4] L. Dalesio, *et al.*, *Proc. of the Intl. Conf. on Accel. and Large Exptl. Phys. Control Systems*, pp. 278-282 (1992).